12-1-2014

Saturated free fatty acids induce cholangiocyte lipoapoptosis

Sathish Kumar Natarajan
University of Nebraska Medical Center, s.natarajan@unmc.edu

Sally A. Ingham
University of Nebraska Medical Center

Ashley M. Mohr
University of Nebraska Medical Center, ashley.mohr@unmc.edu

Cody J. Wehrkamp
University of Nebraska Medical Center, cody.wehrkamp@unmc.edu

Anuttoma Ray
University of Nebraska Medical Center, anuttoma.ray@unmc.edu

See next page for additional authors

Saturated Free Fatty Acids Induce Cholangiocyte Lipoapoptosis

Sathish Kumar Natarajan[1], Sally A. Ingham[1], Ashley M. Mohr[1], Cody J. Wehrkamp[1], Anuttoma Ray[1], Sohini Roy[1], Mary Anne Smith[1], Justin L. Mott[1]

[1]Department of Biochemistry and Molecular Biology,
University of Nebraska Medical Center, Omaha NE

Running title: FFAs induce Cholangiocyte Lipoapoptosis

Address for Correspondence: Justin L. Mott, MD, PhD
Assistant Professor
Department of Biochemistry and Molecular Biology
University of Nebraska Medical Center
985870 Nebraska Medical Center
Omaha, NE 68198-5870
Tel: 402-559-3177
Fax: 402-559-6650
E-mail: justin.mott@unmc.edu

Keywords: bile duct epithelium, forkhead box protein, lipotoxicity, steatohepatitis, steatosis

List of abbreviations: DAPI, 4'-6-diamidino-2-phenylindole; SEM, standard error of the mean; TRAIL, TNF-related apoptosis inducing ligand; PUMA, p53-upregulated modulator of apoptosis; FoxO, forkhead family of transcription factor; JNK, c-Jun N-terminal kinase; MAPK, mitogen activated protein kinase; ERK; extracellular signal-regulated kinase; PBS, phosphate buffered saline; BSA, bovine serum albumin; FBS, fetal bovine serum

The project described was supported by the Fred and Pamela Buffett Cancer Center and the College of Medicine Student Summer Research Program, University of Nebraska Medical Center. The contents of this manuscript are solely the responsibility of the authors.

Number of
- Pages: 27
- Title characters: 61 (incl. spaces)
- Abstract words: 205
- Words with references: 4966
- References: 43
- Figures: 7

ABSTRACT:

Recent studies have identified a cholestatic variant of NAFLD with portal inflammation and ductular reaction. Increased circulating free fatty acids in NAFLD are thought to contribute to injury and disease. Based on reports of biliary damage in NAFLD, we hypothesized the involvement of cholangiocyte lipoapoptosis as a mechanism of cellular injury. Here, we demonstrate that the saturated free fatty acids palmitate and stearate induced robust and rapid cell death in cholangiocytes. Palmitate and stearate induced cholangiocyte lipoapoptosis in a concentration-dependent manner in multiple cholangiocyte-derived cell lines. The mechanism of lipoapoptosis relied on the activation of caspase 3/7 activity. There was also a significant up regulation of the pro-apoptotic BH3-containing protein, PUMA. In addition, palmitate-induced cholangiocyte lipoapoptosis involved a time-dependent increase in the nuclear localization of FoxO3. We show evidence for post-translational modification of FoxO3, including early (6 h) deacetylation and dephosphorylation that coincide with localization of FoxO3 in the nuclear compartment. By 16 h, nuclear FoxO3 is both phosphorylated and acetylated. Interestingly, cultured cholangiocyte-derived cells did not accumulate appreciable amounts of neutral lipid upon free fatty acid treatment. In conclusion, our data show that the saturated free fatty acids palmitate and stearate induce cholangiocyte lipoapoptosis via caspase activation, nuclear translocation of FoxO3 and increased proapoptotic PUMA expression. These results suggest that cholangiocyte injury may occur through lipoapoptosis in NAFLD and NASH patients.

INTRODUCTION

Non-alcoholic fatty liver disease (NAFLD) is the hepatic manifestation of metabolic syndrome (1). NAFLD is a spectrum of liver disease including simple steatosis, non-alcoholic steatohepatitis (NASH), advanced hepatic fibrosis, liver cirrhosis, and hepatocellular carcinoma (1). NAFLD is the most common liver disease among western countries and it is highly associated with obesity, diabetes, dyslipidemia and hypertension (1). Recently, a cholestatic presentation of NAFLD with ductular inflammation, bile duct loss and swelling, and bile duct proliferation was reported (2). They also showed that bridging fibrosis or cirrhosis was more common in patients with biliary injury (2). This suggests the involvement of biliary epithelial cell injury as a possible contributor to the severity of NAFLD or NASH (2, 3). Bile duct epithelial cell expansion, termed the ductular reaction, is a response to injury and has been observed in NAFLD (3). For instance, staining for keratin 19, a biliary epithelial cell marker, was increased in the liver of NAFLD patients containing portal inflammation and advanced fibrosis (3). Furthermore, the increased number of bile ducts in NAFLD with stage 4 fibrosis was due to the proliferation of hepatic bipotential progenitor cells (3). Injured biliary ductular cells produced higher levels of monocyte chemoattractant protein (MCP-1) (3, 4), and increased MCP-1 has been well documented to attract extracellular-matrix producing cells, such as activated myofibroblasts and hepatic stellate cells to the portal traid (3, 4).

NAFLD patients have elevated concentrations of circulating saturated free fatty acids (FFAs). FFA-induced hepatocyte lipoapoptosis is a recognized hallmark of NAFLD and includes the activation of c-Jun N-terminal kinase (JNK), mitogen activated protein

kinase (MAPK) and extracellular signal-regulated kinase (ERK) (5). FFAs have also been shown to induce apoptosis in other cell types like cardiomyocytes (6), and pancreatic β-cells (7). While, hepatocyte lipoapoptosis due to FFAs has been established and implicated in the pathogenesis of NAFLD or NASH (5, 8, 9), the occurrence of cholangiocyte lipoapoptosis due to FFAs has not been thoroughly tested. The present study explores cholangiocyte lipoapoptosis using cholangiocyte cell culture models. The data are consistent with saturated FFA-induced cholangiocyte lipoapoptosis via activation of the forkhead family of transcription factor member, FoxO3 and upregulation of the proapoptotic BH3-containing protein PUMA.

EXPERIMENTAL PROCEDURES

Materials

Palmitic acid (#P5585), stearic acid (#S4751), oleic acid (#O1008) and fatty acid-free bovine serum albumin (BSA); (#A3803) were obtained from Sigma-Aldrich. The pan-caspase inhibitor Z-VAD-fmk was from Santa Cruz (#sc3067) and the JNK inhibitor SP600125 (#420119) was from Calbiochem. Magnetic protein G beads (#S1430S) were purchased from New England Bio Labs.

Antibodies

Rabbit antisera against phospho-FoxO3 (Thr32) (#9464), acetylated-lysine (#9441), FoxO3 (#2497), FoxO1 (#2880), phospho- p38-MAPK (#9211), MAPK (#9212), phospho-ERK1/2 (#9101), ERK1/2, phospho-JNK (#9251), and JNK (#9252) were from Cell Signaling. Rabbit antiserum against PUMA (#ab54288) was from Abcam. Goat anti-Lamin B (#sc-6216) and rabbit anti-actin (#sc-1615) were purchased from Santa Cruz

Biotechnology, Inc. Peroxidase-conjugated secondary antibodies were obtained from Jackson Immuno Research lab.

Cell lines and treatment

H69, a human immortalized cholangiocyte cell line, was grown in Dulbecco's Modified Eagle's Medium (DMEM) supplemented with 10% fetal bovine serum (FBS) and penicillin-streptomycin (100 U/ml), insulin (5 µg/ml), adenine (24.3 µg/ml), epinephrine (1 ug/ml), tri-iodothyronine (T3)- transferrin (T), [T3- 2.23 ng/ml, T-8.19 µg/ml], epidermal growth factor (9.9 ng/ml) and hydrocortisone (5.34 µg/ml). KMCH, Mz-ChA-1 and HuCCT-1, human cholangiocarcinoma cell lines, were grown in DMEM supplemented with 10% FBS, penicillin-streptomycin (100 U/ml), insulin (0.5 µg/ml) and G418 (50 µg/ml). BDEneu cells were a kind gift from Dr. Alphonse Sirica (Virginia Commonwealth Univerisity) and were grown in DMEM supplemented with 10% FBS, penicillin-streptomycin (100 U/ml), human transferrin (5 µg/ml), and insulin (0.5 µg/ml) as described (10). H69, KMCH, HuCCT-1, Mz-ChA-1, and BDEneu cells were treated with the indicated concentrations of FFAs (400-800 µM) dissolved fresh in isopropanol and added to media containing 1% fatty acid-free BSA for 24 h. Vehicle treatment was isopropanol with final concentration of <1% in the medium.

Measurement of apoptosis

Percent apoptosis was quantified by characteristic nuclear morphology and visualized by treatment with the fluorescent DNA-binding dye, DAPI (4', 6-diamidine-2'-phenylindole dihydrochloride) as described before (8). Briefly, cells were stained with 5 µg/ml of DAPI for 20-30 min at 37°C. Apoptotic nuclei (condensed, fragmented) were

counted and presented as a percent of total nuclei. At least 100 cells were counted per well and experiments were performed in triplicate. Caspase 3/7 activity was measured by enzymatic fluorophore release (Apo-One) according to the manufacturer's instructions (Promega) with experiments performed in quadruplicate.

Oil red O staining

Intracellular lipid droplets were stained using oil red O dye as previously described (11). Briefly, cells were treated with 600 μM of the indicated free fatty acids for 24 h. Cells were washed with PBS and fixed with 10% buffered formalin for 10 min. Oil red O (2 mg/ml) staining solution was added for 15 min, and washed with water. Cells were mounted using Fluoromount G (Electron Microscopy Services). Images were obtained by Olympus 1X71 fluorescent microscopy using the rhodamine channel.

Immunoblot and immunofluorescence

Cell lysates containing 25-30 μg of protein were resolved by SDS-PAGE. Proteins were transferred to a nitrocellulose membrane and visualized by immunoblotting. Mz-ChA-1 cells were labeled with anti-FoxO3 antibody and visualized by alexafluor 488 secondary staining.

Nuclear isolation

Cells were rinsed once with ice cold PBS, then scraped in a buffer containing 10 mM 4-(2-hydroxyethyl)piperazine-1-ethanesulfonic acid, (HEPES), pH 7.9, 10 mM KCl, 0.1 mM EDTA, 0.1 mM DTT and 0.5% nonidet-P40 substitute (Sigma) along with the addition of complete protease inhibitor (Roche). Lysates were centrifuged at 15,000 x *g*

for 3 minutes to pellet nuclei. Pellets were suspended in buffer containing 20 mM HEPES, pH 7.9, 0.4 M NaCl, 1 mM EDTA, 0.05 mM DTT, 10 % glycerol and protease inhibitor cocktail and incubated for 40 minutes on ice with occasional vigorous vortexing. Extracts were centrifuged a final time at 15,000 x *g* and probed for FoxO transcription factors.

Statistics

Statistical analysis was performed using one-way analysis of variance (ANOVA) with bonferroni post hoc correction, unless indicated otherwise.

RESULTS

FFAs induced cholangiocyte lipoapoptosis

Biochemical characteristics of apoptosis include nuclear morphology changes and activation of the caspase cascade. We tested the effect of 400, 600, and 800 μM FFAs on cholangiocyte lipoapoptosis. These concentrations were chosen based on circulating levels of total FFAs found in NAFLD or NASH patients (12, 13) and previous studies (5, 8). The saturated FFAs palmitate (PA) and stearate (SA) induced cholangiocytes to undergo lipoapoptosis in a concentration-dependent manner. (Fig 1). Both PA and SA resulted in 25% - 60% apoptosis in H69 cells (Fig 1A). The monounsaturated fatty acid, oleate (OA) showed no apoptosis at 400 μM and 600 μM. In contrast, 800 μM of OA-treated H69 cells showed minimal apoptosis compared with 800 μM of PA-or SA- treated cells. To confirm the apoptotic nuclear changes, we tested the activation of caspase 3/7 in FFA-treated cells. PA and SA treatment of cholangiocytes resulted in significantly increased caspase 3/7 activity in a

concentration-dependent manner. Indeed, 600 μM and 800 μM PA resulted in 4- and 6-fold increased caspase 3/7 activity in H69 cells, whereas 600 μM and 800 μM SA resulted in 5- and 8-fold increased caspase 3/7 activity, respectively (Fig 1A). H69 cells, upon OA treatment again showed a significant increase in caspase activity only at 800 μM OA (Fig 1A). FFA-induced cholangiocyte lipoapoptosis was then tested in additional cholangiocyte-derived cell lines. PA induced an increase in the number of apoptotic nuclei in KMCH cells at 600 μM and 800 μM, whereas SA induced increased lipoapoptosis starting from 400 μM to 800 μM. Increased caspase activity was observed with increasing concentrations of both PA and SA in KMCH cells (Fig 1B). Treatment of KMCH cells with OA did not induce apoptosis (Fig 1B). Both Mz-ChA-1 and HuCCT cell lines showed similar FFA-induced apoptosis with increasing concentrations of PA and SA, but not with OA (Fig 1C & D). Together, these results suggest that saturated FFAs SA and PA induced cholangiocyte lipoapoptosis.

Caspase-dependent cholangiocyte lipoapoptosis

Since caspase activation was observed in FFA-induced cholangiocyte cell death, we tested whether inhibition of caspases using a cell permeable, pan-caspase inhibitor Z-VAD-fmk, would prevent FFA-induced cell death. In KMCH cells, addition of Z-VAD-fmk (50 μM) resulted in complete prevention of caspase 3/7 activity induced by PA and SA treatments (Fig 2A). In parallel, addition of the caspase inhibitor to PA- or SA-treated cells resulted in a significantly decreased percentage of apoptotic nuclei (Fig 2B). In Mz-ChA-1 cells, Z-VAD-fmk treatment also dramatically reduced PA- or SA-induced cell death (Fig 2C). Z-VAD-fmk was also protective against lipoapoptosis in H69 and HuCCT cells (Fig 2D and 2E).

To check the generality of cholangiocyte lipoapoptosis across species, we tested BDEneu cells, an immortalized tumorigenic rat cholangiocyte which has constitutive overexpression of the rat neu/her2 oncogene (10). BDEneu cells treated with vehicle showed 2.39 ± 0.8 percent apoptotic nuclei and 600 μM PA resulted in significantly increased levels of apoptotic nuclei to 35 ± 2.2 percent (Fig 3A). Treatment with caspase inhibitor plus PA significantly decreased the percentage of apoptotic nuclei to 16 ± 0.7. In addition, BDEneu cells treated with 600 μM PA showed a 2.5-fold increase in caspase 3/7 activity, which was blocked by Z-VAD-fmk (Fig 3B).

FFAs induced JNK, ERK1/2 and p38-MAPK activation

Activation of JNK in patients with NAFLD (14) and JNK-dependent hepatocyte lipoapoptosis has been well documented (5, 8). Here we tested whether activation of JNK was also involved in cholangiocyte lipoapoptosis. Indeed, JNK is activated by phosphorylation after 1 h of PA treatment as compared to vehicle-treated KMCH cells. Phospho-JNK levels stayed elevated up to 16 h of PA treatment, with peak activation observed at 8 h of PA (Fig 4A). Similar to JNK activation, PA treatment also resulted in activation of ERK and p38-MAPK via phosphorylation. KMCH cells have some constitutively phosphorylated ERK, as seen in vehicle-treated cells, and 2 h of PA treatment resulted in further activation of ERK. The increase in phospho-ERK levels with PA was time-dependent with peak activation time between 4-8 h (Fig 4A). Increased levels of phospho-p38-MAPK were apparent after 1 h of PA and remained elevated until after 24 h of PA treatment (Fig 4A). PA-induced activation of JNK, ERK and p38-MAPK were also evident in another cholangiocyte, Mz-ChA-1 cells. Here, PA-treated cells showed activation of JNK after 1.5 h of treatment as compared with

vehicle-treated cells and phospho-JNK levels returned to basal levels after 3 h of PA treatment (Fig 4B). Phospho-ERK and phospho-p38-MAPK levels were also increased after 1.5 h of PA treatment and stayed elevated until after 6 h in PA-treated cells. The increased levels of phospho-JNK, phospho-ERK and phospho-p38-MAPK returned to control levels after 8 h of PA treatment in Mz-ChA-1 cells (Fig 4B). JNK was the main MAPK identified to contribute to hepatocyte lipoapoptosis (5). We next tested the small molecule inhibitor for JNK, SP600125, to see whether PA-induced cholangiocyte lipoapoptosis is JNK dependent. Inhibition of JNK did not alter cholangiocyte lipoapoptosis caused by PA in KMCH cells (Fig 4C). Inhibition of JNK was confirmed by the loss of phospho-JNK levels with 50 μM of SP600125 treatment (data not shown). These results suggest that FFAs induced activation of stress kinases JNK, ERK and p38-MAPK and that inhibition of JNK did not alter cholangiocyte lipoapoptosis.

Palmitate induced FoxO3 nuclear localization

We next tested whether FoxO transcription factors (FoxO1 and FoxO3) were involved in palmitate-induced cholangiocyte lipoapoptosis. Nuclear accumulation of FoxO1 and FoxO3 has been shown to induce apoptosis. Nuclear extracts were isolated to analyze FoxO levels in KMCH cells treated with 800 μM of PA. Increased FoxO3 was observed in the nucleus after 3 h of PA as compared to vehicle-treated cells and nuclear FoxO3 levels stayed elevated until after 24 h. Lamin B was used as a loading control (Fig 5A). Nuclear levels of FoxO3 were also increased in H69 and Mz-ChA-1 cells treated with PA for 16 h (Fig 5B). FoxO1 expression in the nuclear extracts was high in H69 cells. However, FoxO1 levels were not altered with PA treatment in either H69 or Mz-ChA-1 cells (Fig 5B). To further confirm nuclear localization, we performed

immunofluorescent analysis for FoxO3 in Mz-ChA-1 cells. FoxO3 is clearly localized to the nucleus after 16 h of PA treatment as compared to the cytosolic staining observed in vehicle-treated cells (Fig 5C). Quantitation of nuclear FoxO3 levels showed a 7-fold increase after 16 h of PA treatment relative to vehicle-treated cells (Fig 5D). In addition to the increased levels of nuclear FoxO3, a slight change in migration of FoxO3 was noted on SDS-PAGE compared to vehicle-treated cells in both H69 and Mz-ChA-1 cells (Fig 5B). This altered migration pattern led us to test the post translational modifications like acetylation and phosphorylation in nuclear extracts from KMCH cells treated with PA. FoxO3 was immunoprecipitated from nuclear extracts and probed using an anti-acetyl-lysine antibody. We observed a dramatic decrease in levels of acetylated FoxO3 (Fig 5E). Note there is no obvious increase in total nuclear FoxO3 in this pull-down experiment; this is likely a technical issue, as Immunoprecipitation is not the most suitable method to detect an increase in total FoxO3 (c.f. Fig 5A). At the same time, FoxO3 was also observed to be un-phosphorylated (Fig 5E). At a later time point, PA treatment of HuCCT and H69 cells resulted in an increase in the levels of acetylated FoxO3 and phosphorylated FoxO3 (Fig 5F). These results suggest that FoxO3 was deacetylated and dephosphorylated at early time points, when it first translocated to the nucleus, and at the later time points, FoxO3 is getting modified via acetylation and phosphorylation.

Palmitate increases PUMA protein expression in cholangiocytes

PUMA is a downstream target of FoxO3 (15), thus we assessed the expression of PUMA protein in KMCH cells at various time points after treatment with 800 μM PA.

PA-treated KMCH cells showed elevated levels of PUMA after 2 h as compared to 0 h treated cells and the increased PUMA levels were sustained even after 48 h (Fig 6).

Cholangiocytes do not develop steatosis with FFA treatment

Treatment of hepatocytes with FFAs was previously shown to increase lipid storage as triglycerides in cytoplasmic lipid droplets (5). We tested cholangiocytes such as H69, Mz-ChA-1, KMCH and hepatoma cells, Huh7 for lipid droplet formation after treatment with 600 μM PA, SA, or OA by staining with oil red O dye. H69 cells showed background of minimal lipid droplet staining and this did not increase with PA or SA treatment, whereas OA-treated cells showed a slight increase in lipid droplet formation (Fig 7). Mz-ChA-1 and KMCH cells did not show accumulation of lipid droplets with 600 μM of PA, SA, or OA treatment after 24 h. In contrast to cholangiocytes, Huh7 hepatoma cells showed a dramatic increase in the accumulation of lipid droplets with all of the FFAs. These results suggest that cholangiocytes do not develop steatosis, in contrast to hepatocytes.

DISCUSSION

Circulating saturated FFAs are reported to be elevated in patients with metabolic syndrome as well as in patients with NAFLD or NASH (12, 13). The principal finding of this study is that FFAs can induce biliary epithelial cell lipoapoptosis. Our data suggest four important findings in biliary cell damage induced by FFAs, termed cholangiocyte lipoapoptosis: a) FFAs induced caspase activation and cholangiocyte apoptosis; b) cholangiocyte lipoapoptosis was associated with the activation of FoxO3, a transcription factor known to induce apoptosis; c) cholangiocyte lipoapoptosis appears to involve the

activation of PUMA, a proapoptotic BH3-containing protein; and d) unlike hepatocytes, cholangiocytes did not accumulate lipid droplets. These results will be discussed below.

Are cholangiocyte cell culture models, a clinically relevant model to study biliary epithelial cell lipoapoptosis? In the present study, we used normal immortalized cholangiocyte cell line, H69 and cholangiocarcinoma-derived cell lines, KMCH, Mz-ChA-1, and HuCCT. H69 cells have been shown to contain similar characteristics to human primary cholangiocytes. H69 cells can produce primary cilia from the apical plasma membrane during *in vitro* culture conditions(16). Both normal cholangiocytes and cholangiocarcinoma-derived cell lines used in this study were shown to express keratin 7, keratin 19, and gamma-glutamyl transpeptidase activity, similar to cholangiocytes *in vivo* and primary human cholangiocytes (17, 18). Additionally, both Mz-ChA-1 cells and normal cholangiocytes express HMG-CoA reductase (19). Thus, the cell lines employed in the current study share phenotypic features with biliary epithelial cells and are a useful culture model of cholangiocytes.

Saturated FFAs, like PA and SA have been shown to cause lipotoxicity and induce lipoapoptosis due to the activation of caspases in various mammalian cells including pancreatic β-cells (7), cardiomyocytes (20), and hepatocytes (5, 8)and other cell types. Hepatocytes and cholangiocytes have a common precursor cell, termed the bipotential hepatic progenitor cell (21). In the present study, we report lipotoxicity due to saturated FFAs in biliary epithelial cells. This is a caspase-dependent process, consistent with previous studies in other cell types. The monounsaturated fatty acid, OA, showed slight toxicity at the highest concentration. This agrees with a previous study in which OA-induced lipotoxicity in renal proximal tubule cells (22). Treatment with

a pan-caspase inhibitor protected against cholangiocyte lipoapoptosis caused by saturated FFAs. Biliary injury has been reported in a subset of patients with NAFLD compared to a population with similar steatosis (2, 3). Our data suggest that in patients with metabolic syndrome, higher circulating FFAs may contribute to biliary tree damage. Further studies will be needed to determine if cholangiocyte lipoapoptosis contributes to the progression of disease from simple steatosis to NASH to liver fibrosis, at least in a subset of patients.

JNK is one of the major cellular stress signaling kinases that is activated during FFA-induced apoptosis. In particular, hepatocyte lipoapoptosis is dependent on JNK activation (5, 8). However, we found that inhibition of JNK using a small molecule inhibitor did not prevent cholangiocyte lipoapoptosis, suggesting a mechanism of apoptosis beyond JNK activation. A recent study in pancreatic β-cells showed that FFA-induced JNK activation is not critical for apoptosis; but JNK activation was involved in mediating ER-stress signaling pathways (7). Several studies have also demonstrated that p38-MAPK and ERK can also induce apoptosis in pancreatic β-cells (23, 24), but the activation of p38-MAPK and ERK has been shown not to be critical for FFA-induced hepatocyte lipoapoptosis (5).

Since JNK was not a critical mediator of FFA-induced cholangiocyte lipoapoptosis, our focus was next on FoxO3. FoxO3, a forkhead family transcription factor, has been shown to activate cell death pathways by inducing the expression of proapoptotic proteins such as PUMA, Bim, p27, and TRAIL (6, 15). Several studies have confirmed that FoxO3 has direct transcriptional activity on the PUMA promoter and induces the expression of PUMA protein (15, 25). Increased PUMA can also induce Bax

and Bak oligomerization, which further results in activating mitochondrial intrinsic pathways of apoptosis by releasing cytochrome *c* resulting in caspase activation (26). FoxO3 can also be regulated by the Akt signaling pathway, protein phosphatases, and protein deacetylases (Sirt1) (27-29). Phosphorylation and acetylation of FoxO3 have been shown to alter the cell death pathways towards cell survival by promoting export of FoxO3 from the nucleus to the cytoplasm (27). Sirt1 interacts with FoxO3 in the nucleus resulting in deacetylation and altered transcriptional activity (30). In the present study, deacetylation and dephosphorylation of FoxO3 were observed at the early time points after PA treatment in KMCH cells. After 16 h of PA treatment, the levels of acetylated FoxO3 and phosphorylated FoxO3 were increased. Although phosphorylation has been reported to promote nuclear export, we observed increased nuclear localization of FoxO3 even after 16h of PA. We conclude that in PA-treated cholangiocytes, phosphorylation of FoxO3 at Thr32 is not sufficient to cause nuclear export and FoxO3 inactivation. Previously, PA has been shown to decrease the expression of Sirt1 in pancreatic β-cells (31) and cardiomyocytes (20). Overexpression of Sirt1 has been shown to protect against FFA-induced pancreatic β-cell apoptosis (32). Consistently, acetylated FoxO1 has been shown to induce Bim expression and promote apoptosis (33). FFAs have been shown to induce the expression of miR-195 and miR-34a in cardiomyocytes and pancreatic β-cells, respectively, and both miR-195 and miR-34a have been shown to target Sirt1, resulting in an increase in the acetylated form of transcription factors (34). At present, we cannot exclude the possibility of microRNA regulation of FFA-induced cholangiocyte lipoapoptosis, which merits our future investigation.

As noted, PUMA is important in lipoapoptosis, and is a downstream target of FoxO3 (15). Expression of PUMA was found to be up-regulated in human liver biopsies taken from NASH patients as compared to control subjects (8). In our experiments, PUMA expression was up regulated by FFAs in cholangiocytes. Our time-course of PUMA expression revealed a rapid increase in PUMA protein that is sustained through 48 h. Because of the rapid induction, it is likely the early increase is due, in part, to post-transcriptional mechanisms. The sustained increase in expression may be the result of FoxO3-mediated transcriptional activation or alternate signaling mechanisms.

Furthermore, we measured cellular steatosis, i.e., accumulation of triglycerides in lipid droplets, which has been reported in many non-adipose tissues including pancreatic β-cells, cardiomyocytes, and hepatocytes (5, 35). In the liver, there is controversy over whether lipid droplets in hepatocytes treated with FFAs promote lipotoxicity or serve as a protective mechanism for detoxifying FFAs (35-40). In the present study, FFA treatment of cholangiocytes did not induce cellular steatosis. These results are consistent with the clinical observation of hepatocyte lipid accumulation without biliary cell steatosis in NAFLD (41-43). Lipid droplet accumulation in cholangiocytes has been reported in mice with liver-specific deficiency of adipose triglyceride lipase (ATGL), a major lipase in cholangiocytes (21). Together, cholangiocytes undergo lipoapoptosis with FFA treatment, but unlike hepatocytes, cholangiocytes did not accumulate lipid droplets with FFA treatment.

In conclusion, our study shows that saturated FFAs induce cholangiocyte lipoapoptosis via caspase activation, nuclear translocation of FoxO3 and proapoptotic PUMA expression. Post-translational modifications of FoxO3 may be involved in

cholangiocyte lipoapoptosis. Further studies are required to elucidate the contribution of cholangiocyte lipoapoptosis to NAFLD or NASH patients with metabolic syndrome.

Acknowledgements

We would like to acknowledge Crystal Cordes and John Davis for their help with oil red O staining. We thank Carol Casey for the helpful discussions and Sophie Cazanave for sharing her expertise and FFA treatment protocols.

REFERENCE

1. Ibrahim SH, Kohli R, Gores GJ. Mechanisms of lipotoxicity in NAFLD and clinical implications. J Pediatr Gastroenterol Nutr 2011;53:131-140.

2. Sorrentino P, Tarantino G, Perrella A, Micheli P, Perrella O, Conca P. A clinical-morphological study on cholestatic presentation of nonalcoholic fatty liver disease. Dig Dis Sci 2005;50:1130-1135.

3. Chiba M, Sasaki M, Kitamura S, Ikeda H, Sato Y, Nakanuma Y. Participation of bile ductular cells in the pathological progression of non-alcoholic fatty liver disease. J Clin Pathol 2011;64:564-570.

4. Harada K, Chiba M, Okamura A, Hsu M, Sato Y, Igarashi S, Ren XS, et al. Monocyte chemoattractant protein-1 derived from biliary innate immunity contributes to hepatic fibrogenesis. J Clin Pathol 2011;64:660-665.

5. Malhi H, Bronk SF, Werneburg NW, Gores GJ. Free fatty acids induce JNK-dependent hepatocyte lipoapoptosis. J Biol Chem 2006;281:12093-12101.

6. Barreyro FJ, Kobayashi S, Bronk SF, Werneburg NW, Malhi H, Gores GJ. Transcriptional regulation of Bim by FoxO3A mediates hepatocyte lipoapoptosis. J Biol Chem 2007;282:27141-27154.

7. Nemcova-Furstova V, Balusikova K, Sramek J, James RF, Kovar J. Caspase-2 and JNK activated by saturated fatty acids are not involved in apoptosis induction but modulate ER stress in human pancreatic beta-cells. Cell Physiol Biochem 2013;31:277-289.

8. Cazanave SC, Mott JL, Elmi NA, Bronk SF, Werneburg NW, Akazawa Y, Kahraman A, et al. JNK1-dependent PUMA expression contributes to hepatocyte lipoapoptosis. J Biol Chem 2009;284:26591-26602.

9. Akazawa Y, Guicciardi ME, Cazanave SC, Bronk SF, Werneburg NW, Kakisaka K, Nakao K, et al. Degradation of cIAPs Contributes to Hepatocyte Lipoapoptosis. Am J Physiol Gastrointest Liver Physiol 2013.

10. Sirica AE, Zhang Z, Lai GH, Asano T, Shen XN, Ward DJ, Mahatme A, et al. A novel "patient-like" model of cholangiocarcinoma progression based on bile duct inoculation of tumorigenic rat cholangiocyte cell lines. Hepatology 2008;47:1178-1190.

11. Schadinger SE, Bucher NL, Schreiber BM, Farmer SR. PPARgamma2 regulates lipogenesis and lipid accumulation in steatotic hepatocytes. Am J Physiol Endocrinol Metab 2005;288:E1195-1205.

12. Nehra V, Angulo P, Buchman AL, Lindor KD. Nutritional and metabolic considerations in the etiology of nonalcoholic steatohepatitis. Dig Dis Sci 2001;46:2347-2352.

13. Bechmann LP, Kocabayoglu P, Sowa JP, Sydor S, Best J, Schlattjan M, Beilfuss A, et al. Free fatty acids repress small heterodimer partner (SHP) activation and adiponectin counteracts bile acid-induced liver injury in superobese patients with nonalcoholic steatohepatitis. Hepatology 2013;57:1394-1406.

14. Ferreira DM, Castro RE, Machado MV, Evangelista T, Silvestre A, Costa A, Coutinho J, et al. Apoptosis and insulin resistance in liver and peripheral tissues of morbidly obese patients is associated with different stages of non-alcoholic fatty liver disease. Diabetologia 2011;54:1788-1798.

15. You H, Pellegrini M, Tsuchihara K, Yamamoto K, Hacker G, Erlacher M, Villunger A, et al. FOXO3a-dependent regulation of Puma in response to cytokine/growth factor withdrawal. J Exp Med 2006;203:1657-1663.

16. Masyuk AI, Huang BQ, Radtke BN, Gajdos GB, Splinter PL, Masyuk TV, Gradilone SA, et al. Ciliary subcellular localization of TGR5 determines the cholangiocyte functional response to bile acid signaling. Am J Physiol Gastrointest Liver Physiol 2013;304:G1013-1024.

17. Humphreys EH, Williams KT, Adams DH, Afford SC. Primary and malignant cholangiocytes undergo CD40 mediated Fas dependent apoptosis, but are insensitive to direct activation with exogenous Fas ligand. PLoS One 2010;5:e14037.

18. Harnois DM, Que FG, Celli A, LaRusso NF, Gores GJ. Bcl-2 is overexpressed and alters the threshold for apoptosis in a cholangiocarcinoma cell line. Hepatology 1997;26:884-890.

19. Miller T, Yang F, Wise CE, Meng F, Priester S, Munshi MK, Guerrier M, et al. Simvastatin stimulates apoptosis in cholangiocarcinoma by inhibition of Rac1 activity. Dig Liver Dis 2011;43:395-403.

20. Zhu H, Yang Y, Wang Y, Li J, Schiller PW, Peng T. MicroRNA-195 promotes palmitate-induced apoptosis in cardiomyocytes by down-regulating Sirt1. Cardiovasc Res 2011;92:75-84.

21. Wu JW, Wang SP, Alvarez F, Casavant S, Gauthier N, Abed L, Soni KG, et al. Deficiency of liver adipose triglyceride lipase in mice causes progressive hepatic steatosis. Hepatology 2011;54:122-132.

22. Arany I, Clark JS, Reed DK, Juncos LA, Dixit M. Role of p66shc in Renal Toxicity of Oleic Acid. Am J Nephrol 2013;38:226-232.

23. Yuan H, Zhang X, Huang X, Lu Y, Tang W, Man Y, Wang S, et al. NADPH oxidase 2-derived reactive oxygen species mediate FFAs-induced dysfunction and apoptosis of beta-cells via JNK, p38 MAPK and p53 pathways. PLoS One 2010;5:e15726.

24. Kim K, Park M, Young Kim H. Ginsenoside Rg3 Suppresses Palmitate-Induced Apoptosis in MIN6N8 Pancreatic beta-Cells. J Clin Biochem Nutr 2010;46:30-35.

25. Amente S, Zhang J, Lavadera ML, Lania L, Avvedimento EV, Majello B. Myc and PI3K/AKT signaling cooperatively repress FOXO3a-dependent PUMA and GADD45a gene expression. Nucleic Acids Res 2011;39:9498-9507.

26. Natarajan SK, Becker DF. Role of apoptosis-inducing factor, proline dehydrogenase, and NADPH oxidase in apoptosis and oxidative stress. Cell Health Cytoskelet 2012;2012:11-27.

27. Natarajan SK, Zhu W, Liang X, Zhang L, Demers AJ, Zimmerman MC, Simpson MA, et al. Proline dehydrogenase is essential for proline protection against hydrogen peroxide-induced cell death. Free Radic Biol Med 2012;53:1181-1191.

28. Ni YG, Wang N, Cao DJ, Sachan N, Morris DJ, Gerard RD, Kuro OM, et al. FoxO transcription factors activate Akt and attenuate insulin signaling in heart by inhibiting protein phosphatases. Proc Natl Acad Sci U S A 2007;104:20517-20522.

29. Wang F, Chan CH, Chen K, Guan X, Lin HK, Tong Q. Deacetylation of FOXO3 by SIRT1 or SIRT2 leads to Skp2-mediated FOXO3 ubiquitination and degradation. Oncogene 2012;31:1546-1557.

30. Brunet A, Sweeney LB, Sturgill JF, Chua KF, Greer PL, Lin Y, Tran H, et al. Stress-dependent regulation of FOXO transcription factors by the SIRT1 deacetylase. Science 2004;303:2011-2015.

31. Wu L, Zhou L, Lu Y, Zhang J, Jian F, Liu Y, Li F, et al. Activation of SIRT1 protects pancreatic beta-cells against palmitate-induced dysfunction. Biochim Biophys Acta 2012;1822:1815-1825.

32. Lee JH, Song MY, Song EK, Kim EK, Moon WS, Han MK, Park JW, et al. Overexpression of SIRT1 protects pancreatic beta-cells against cytokine toxicity by suppressing the nuclear factor-kappaB signaling pathway. Diabetes 2009;58:344-351.

33. Yang Y, Zhao Y, Liao W, Yang J, Wu L, Zheng Z, Yu Y, et al. Acetylation of FoxO1 activates Bim expression to induce apoptosis in response to histone deacetylase inhibitor depsipeptide treatment. Neoplasia 2009;11:313-324.

34. Yamakuchi M, Ferlito M, Lowenstein CJ. miR-34a repression of SIRT1 regulates apoptosis. Proc Natl Acad Sci U S A 2008;105:13421-13426.

35. Dong ML, Ding XZ, Adrian TE. Red oil A5 inhibits proliferation and induces apoptosis in pancreatic cancer cells. World J Gastroenterol 2004;10:105-111.

36. Malhi H, Gores GJ. Molecular mechanisms of lipotoxicity in nonalcoholic fatty liver disease. Semin Liver Dis 2008;28:360-369.

37. Listenberger LL, Han X, Lewis SE, Cases S, Farese RV, Jr., Ory DS, Schaffer JE. Triglyceride accumulation protects against fatty acid-induced lipotoxicity. Proc Natl Acad Sci U S A 2003;100:3077-3082.

38. Neuschwander-Tetri BA. Hepatic lipotoxicity and the pathogenesis of nonalcoholic steatohepatitis: the central role of nontriglyceride fatty acid metabolites. Hepatology 2010;52:774-788.

39. Yamaguchi K, Yang L, McCall S, Huang J, Yu XX, Pandey SK, Bhanot S, et al. Inhibiting triglyceride synthesis improves hepatic steatosis but exacerbates liver damage and fibrosis in obese mice with nonalcoholic steatohepatitis. Hepatology 2007;45:1366-1374.

40. Wang H, Sreenevasan U, Hu H, Saladino A, Polster BM, Lund LM, Gong DW, et al. Perilipin 5, a lipid droplet-associated protein, provides physical and metabolic linkage to mitochondria. J Lipid Res 2011;52:2159-2168.

41. Xanthakos S, Miles L, Bucuvalas J, Daniels S, Garcia V, Inge T. Histologic spectrum of nonalcoholic fatty liver disease in morbidly obese adolescents. Clin Gastroenterol Hepatol 2006;4:226-232.

42. Contos MJ, Choudhury J, Mills AS, Sanyal AJ. The histologic spectrum of nonalcoholic fatty liver disease. Clin Liver Dis 2004;8:481-500, vii.

43. Mofrad P, Contos MJ, Haque M, Sargeant C, Fisher RA, Luketic VA, Sterling RK, et al. Clinical and histologic spectrum of nonalcoholic fatty liver disease associated with normal ALT values. Hepatology 2003;37:1286-1292.

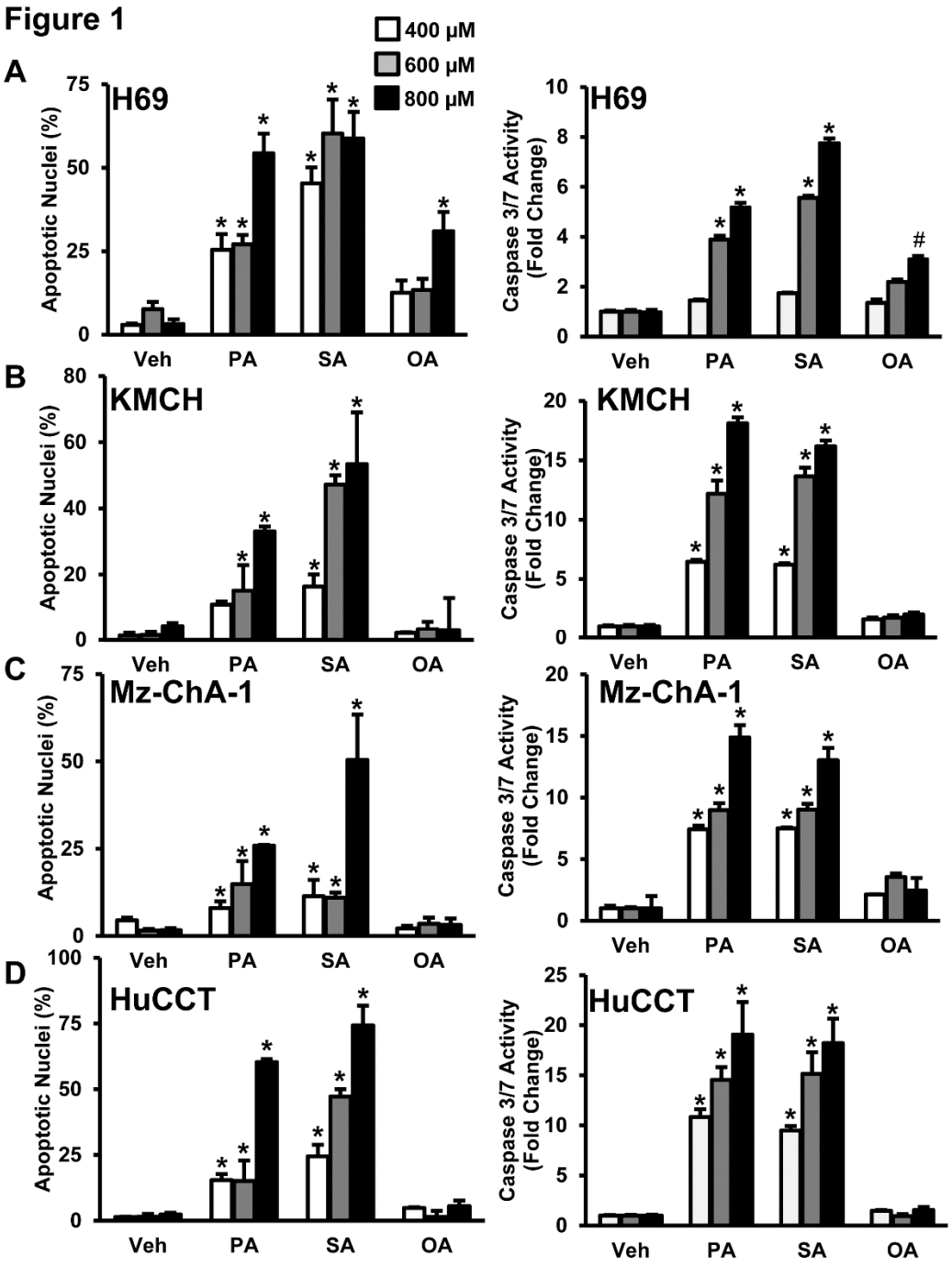

Fig 1. **Free fatty acids induce cholangiocyte lipoapoptosis. (A)** H69 cells were treated with 400, 600, or 800 µM palmitate (PA), stearate (SA) or oleate (OA) for 24 h. Apoptotic nuclei were counted and expressed as a percent of total nuclei *(left panel)*. H69 cells were treated in parallel as above for 24 h, followed by quantitation of caspase 3/7 activity *(right panel)*, and results are expressed as fold-change over isopropanol-treated cells (Veh). The same conditions were employed to assess apoptotic nuclei and caspase 3/7 activity in KMCH cells **(B)**, Mz-ChA-1 cells **(C)**, and HuCCT cells **(D)**. Each value represents the mean ± SEM of separate experiments (n = 6). *p<0.001 and #p<0.05, compared to vehicle-treated cells.

Figure 2

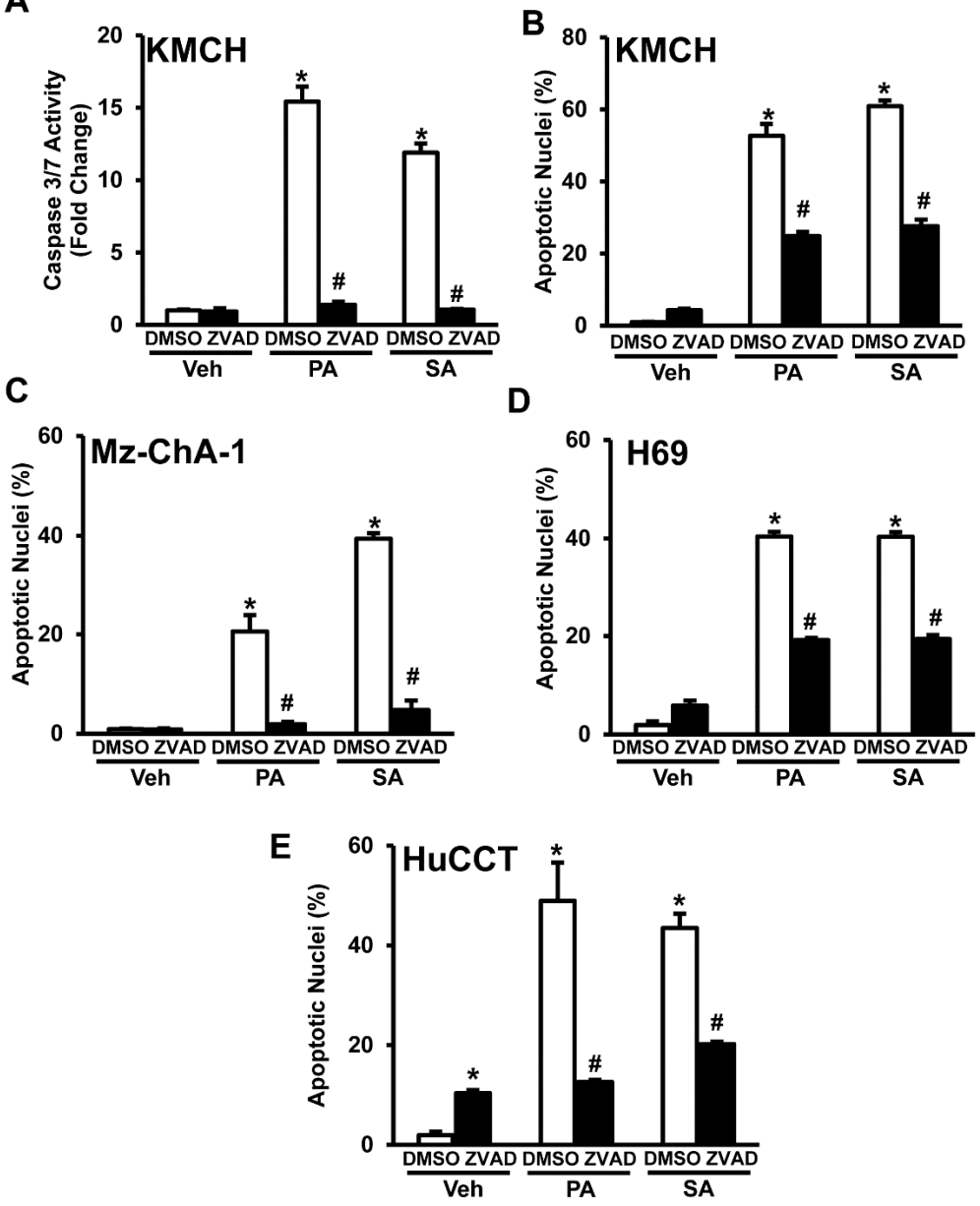

Fig 2. **Caspase-dependent cholangiocyte lipoapoptosis. (A)** KMCH cells were treated for 24 h with 800 μM palmitate (PA) or stearate (SA), and 50 μM caspase inhibitor, Z-VAD-fmk (ZVAD) or DMSO as a control. Results are expressed as fold change of caspase 3/7 activity compared to vehicle treatment (Veh). **(B)** KMCH cells were treated in parallel as above for 24 h, followed by measurement of apoptotic nuclei. Apoptotic nuclei were counted and expressed as a percent of total nuclei*;* at least 100 cells per replicate were counted. The same conditions were employed to assess apoptotic nuclei in Mz-ChA-1 cells **(C)**, H69 cells **(D)**, and HuCCT cells **(E)**. Each value represents mean ± SEM of separate experiments (n = 6). *p<0.001, compared to vehicle, #p<0.05, compared to 800 μM PA or SA treated cells.

Figure 3

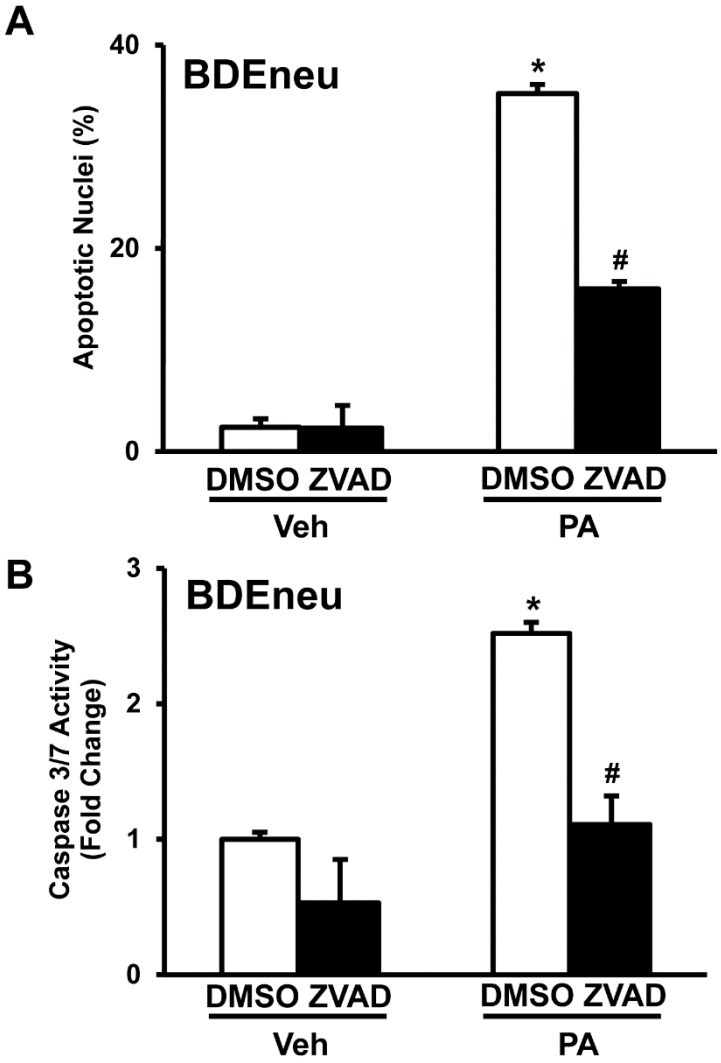

Fig 3. **FFA-induced rat cholangiocyte lipoapoptosis was also caspase dependent. (A)** BDEneu cells were treated with 600 μM palmitate (PA) or PA plus 50 μM caspase inhibitor, Z-VAD-fmk (ZVAD) for 24 h. Vehicle for PA was isopropanol (Veh' <1% final) and control for Z-VAD-fmk was DMSO (<1% final). Apoptotic nuclei were counted and expressed as a percent of total nuclei, at least 100 cells per replicate were counted. **(B)** BDEneu cells were treated in parallel as above for 24 h, followed by quantitation of caspase 3/7 activity, and results are expressed as fold-change over isopropanol-treated cells (Veh). Each value represents the mean ± SEM of separate experiments (n = 6). *p<0.001, compared to vehicle treated cells and #p<0.001 compared to PA-treated cells.

Figure 4

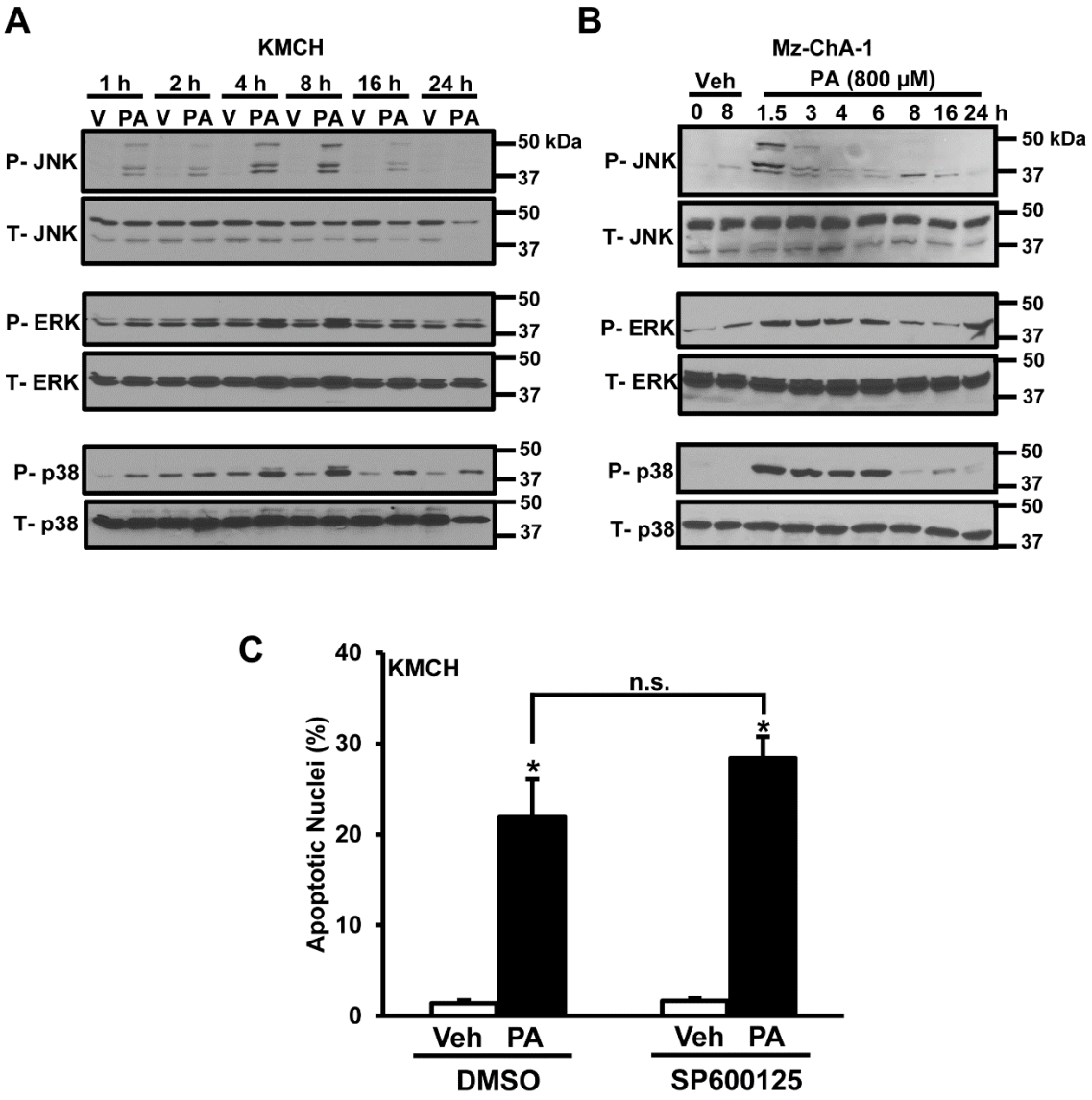

Fig 4**. FFAs induced JNK, ERK1/2 and p38-MAPK activation. (A)** Cell lysates were prepared from KMCH cells treated with either 800 μM palmitate (PA) or vehicle (V) for different time points. Immunoblot analysis was performed for phospho-JNK (P- JNK), phospho-ERK (P- ERK), and phospho-p38-MAPK (P-p38), and compared with total JNK (T-JNK), total ERK (T-ERK) and total p38-MAPK (T-p38), respectively. **(B)** Mz-ChA-1 cells were treated with either 800 μM PA (PA) or vehicle (V), for different time points. Immunoblot analysis was performed in Mz-ChA-1 cells for phosphorylated proteins, and compared with total JNK, ERK, and p38, respectively. The images shown here are representative images. **(C)** KMCH cells were treated with vehicle (Veh) or 800 μM palmitate (PA), with or without 50 μM SP600125 24 h. Apoptotic nuclei were counted and expressed as a percent of total nuclei*,* at least 100 cells per replicate were counted. Each value represents the mean ± SEM of separate experiments (n = 6). *p<0.001, compared to vehicle treated cells and n.s., non-significant.

Figure 5

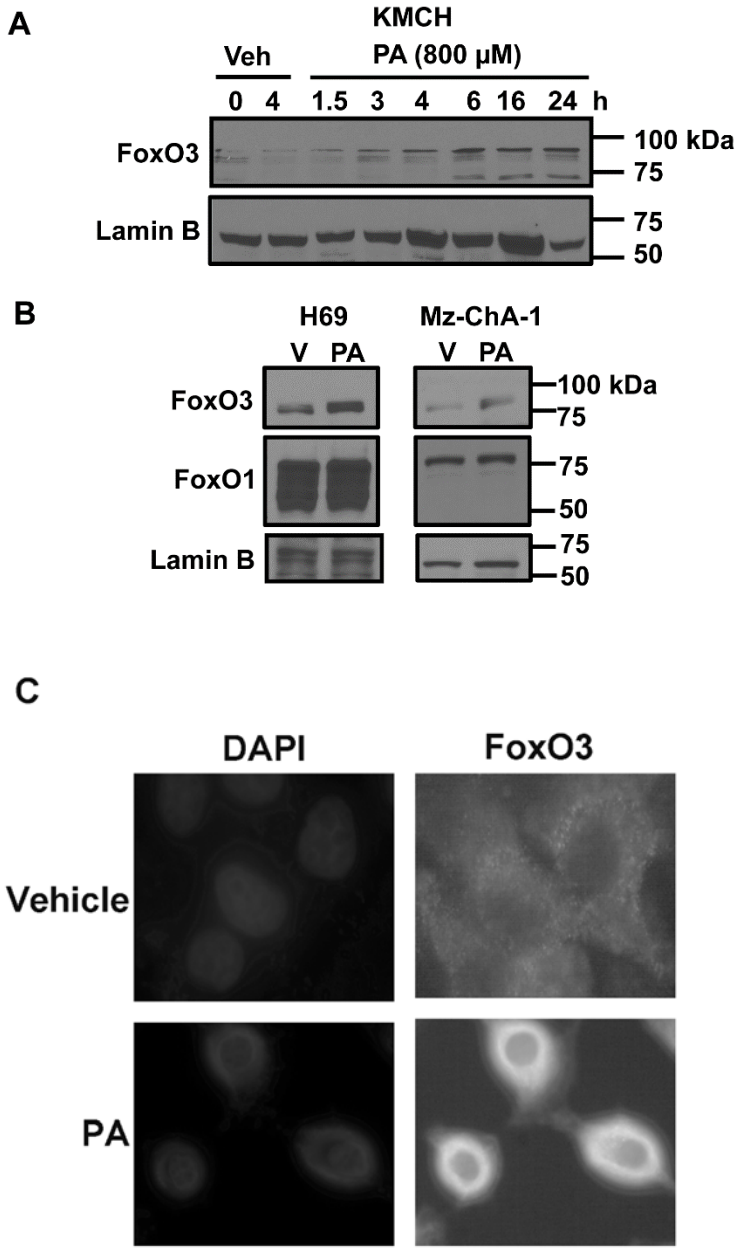
A
KMCH
Veh
PA (800 μM)
0 4 1.5 3 4 6 16 24 h
FoxO3
Lamin B
100 kDa
75
75
50
B
H69
Mz-ChA-1
V PA
V PA
FoxO3
FoxO1
Lamin B
100 kDa
75
75
50
75
50
C
DAPI
FoxO3
Vehicle
PA

Figure 5

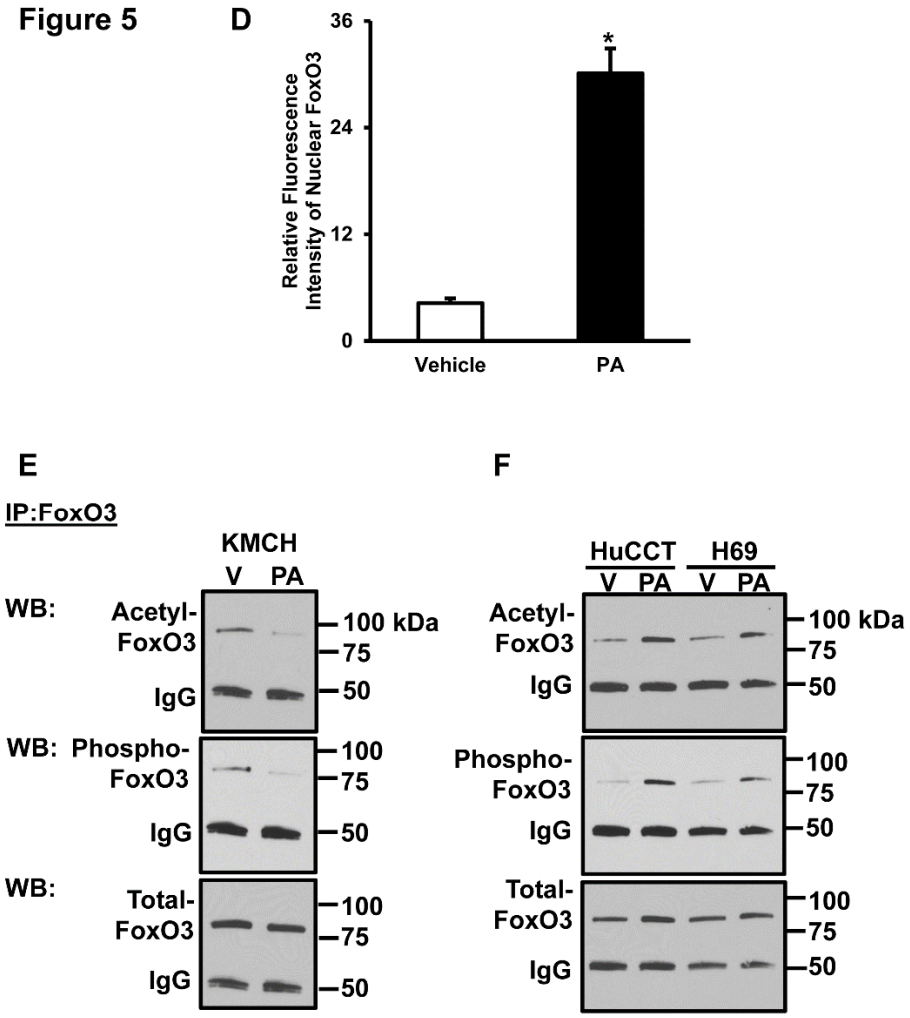

Fig 5**. Palmitate induced FoxO3 nuclear localization. (A)** Nuclear extracts were prepared from KMCH cells treated with either 800 μM palmitate (PA) at different time points or vehicle (Veh) for the indicated times. Immunoblot analysis was performed for FoxO3 and Lamin B was used as a loading control. **(B)** H69 and Mz-ChA-1 cells were treated with 800 μM palmitate (PA) or vehicle (V) for 16 h. Nuclear extracts were analyzed for FoxO3, FoxO1, and Lamin B as a control. **(C)** Immunofluorescence analysis of FoxO3 nuclear localization after 16 h of 800 μM palmitate (PA) or vehicle treatment in Mz-ChA-1 cells and nuclei were counter stained with DAPI. **(D)** Quantified levels of nuclear FoxO3 after 16 h of 800 μM palmitate (PA) or vehicle treatment in Mz-ChA-1 cells. Relative fluorescent intensity was quantified using ImageJ software. Atleast 30 cells were quantified per treatment conditions. *p<0.001 compared to vehicle-treated cells, students *t*-test. **(E)** Immunoprecipitation of total FoxO3 from nuclear extracts of KMCH cells treated with palmitate (PA) or vehicle (V), for 6 h. Immunoblot analysis was performed for acetylated FoxO3, phospho-FoxO3 and total FoxO3. Heavy chain of the IP antibody is indicated as IgG. **(F)** Immunoprecipitation of total FoxO3 from nuclear extracts of HuCCT, and H69 cells treated with 800 μM palmitate (PA) or vehicle (V) for 16 h. Immunoblot analysis was performed for acetylated FoxO3, phospho-FoxO3 and total FoxO3. The images shown here are representative images.

Figure 6

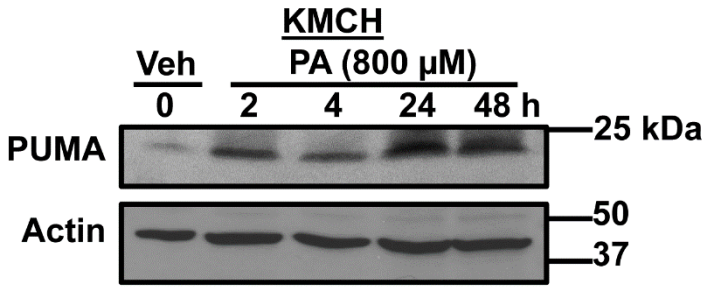

Fig 6. **Palmitate increased PUMA protein expression in cholangiocytes.** KMCH cells were treated with 800 μM palmitate (PA) or vehicle (Veh). Cell lysates were collected at different time points after PA treatment, as indicated. Immunoblot analysis was performed for PUMA and actin was used as a loading control.

Figure 7

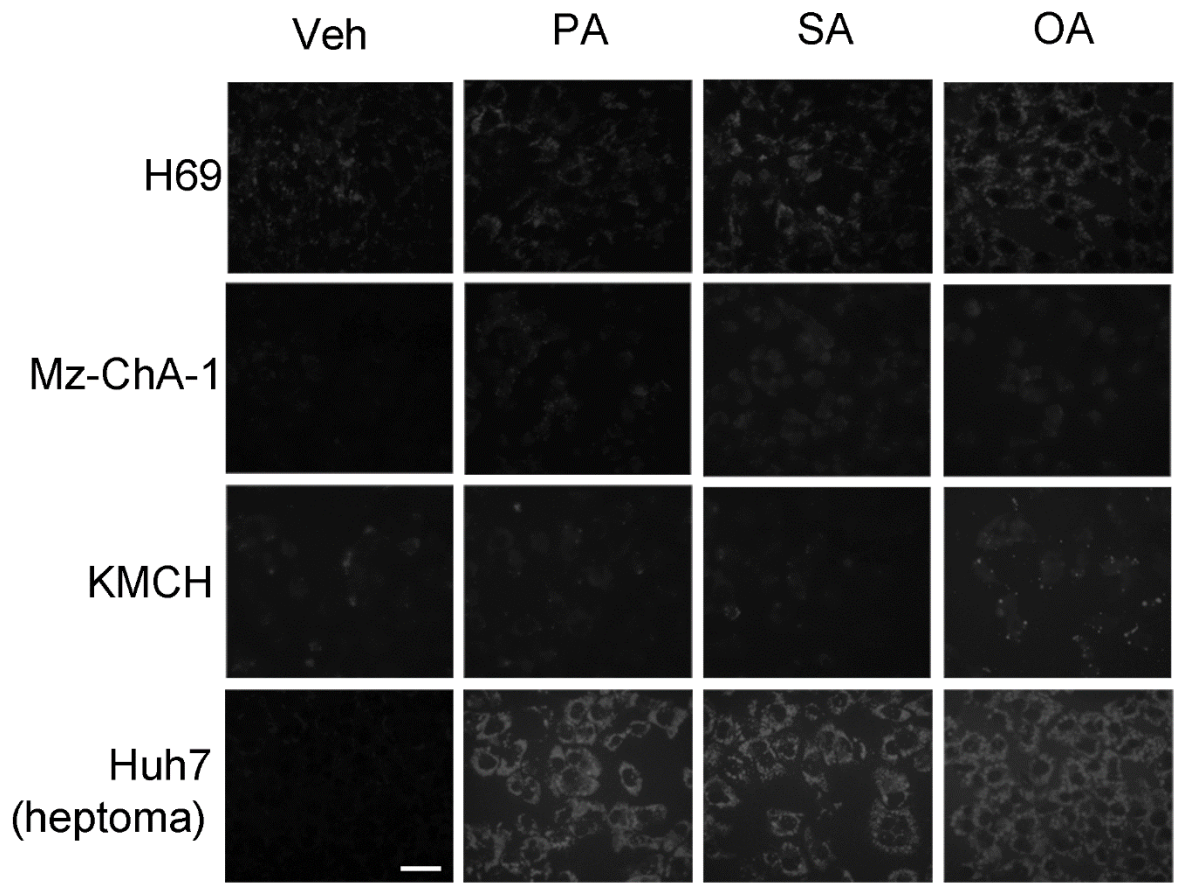

Fig 7. **Cholangiocytes do not develop steatosis with saturated free fatty acid treatment.** H69, Mz-ChA-1, KMCH cholangiocytes or Huh7 hepatoma cells were treated with 600 μM palmitate (PA), stearate (SA), or oleate (OA) for 24 h. Vehicle-treated cells were used as control (Veh). Red fluorescence was captured and images are displayed in greyscale. The images shown here are representative images and all micrographs were taken at the same magnification (bar = 25 μm).